JOURNAL OF MATERIALS SCIENCE **38** (2003) 1523–1528

Cofiring properties and camber development of ferroelectric/ferrite multilayer composites

GAO FENG*, YANG ZUPEI, HOU YUDONG, TIAN CHANGSHENG
Department of Material Science and Engineering, Northwestern Polytechnical University, Xi'an, 710072, People's Republic of China
E-mail: tiancs@nwpu.edu.cn

QU SHAOBO
The college of Mechanical Engineering, Xi'an Jiaotong University, Xi'an, 710049, People's Republic of China

The multilayer ferroelectric/ferrite composites were prepared and their interaction, camber development, and interface microstructure were investigated. The results show that no chemical reaction between the ferroelectrics and ferrite materials existed. The camber is because of a mismatch shrinkage of the composites and were observed at the temperature range from 800°C to 900°C. A simple model was established to describe camber. The investigation of camber development showed that the camber developed firstly toward ferrite and then toward ferroelectrics, finally the composites become flat at 950°C. The multilayer ferroelectric/ferrite composites can be cofired at 950°C and the interface is continuous with no delamination and cracks.

1. Introduction

To keep up with the rapid development of surface mount technology (SMT), some cofired devices such as ceramic filled glass electronic package and varistor-capacitor cofired multilayer devices, have been developed for an increasingly trend of compact design [1, 2]. Multilayer chip LC filter, which is combined with several capacitors and inductors by the production process of multilayer chip components, is a type of advanced surface mount devices (SMD) [3, 4]. Lead based ferroelectrics, such as $Pb(Mg_{1/3}Nb_{2/3})O_3$, $Pb(Ni_{1/3}Nb_{2/3})O_3$ and $Pb(Zn_{1/3}Nb_{2/3})O_3$, are being widely researched as a potential multilayer ceramic capacitor (MLCC) due to their high dielectric constant and low sintering temperature [5–7]. The NiCuZn ferrite with excellent magnetic permeability can also be densified at low temperature, and is an important material using for producing low temperature sintered multilayer chip inductor (MLCI) [8–10]. They two are promising materials for the multilayer chip LC filters.

The key issue of manufacturing the multilayer chip LC filters is cofiring the capacitor and inductor together at low temperature. Because of mismatched firing kinetics between *L* (ferrite) and *C* (dielectric) materials, undesirable cofiring defects including delamination, cracks, and camber are easily introduced in the final products [11]. To minimize the possibility of forming cofiring defects, a more thorough understanding of the above defects is needed before the processing parameters and material compositions are optimized.

The cofiring kinetics and the camber between the inner electrode and ceramics have been widely investigated [12, 13]. But the cofiring densification properties between the capacitor materials and inductor materials, especially the ferroelectrics and ferrite, have not been reported. Furthermore, it is necessary to understand the camber mechanism and interfacial interactions such as chemical reaction, ionic interdiffusion of cofired ferroelectric/ferrite composites.

In the present study, the multilayer composites were prepared by cofiring $Pb(Ni_{1/3}Nb_{2/3})O_3$-$PbTiO_3$-$Pb(Zn_{1/2}W_{1/2})O_3$ ferroelectrics and NiCuZn ferrite. The densification characteristics of single ferroelectrics and ferrite were analyzed first, then cofiring properties involved chemical reaction, camber development, interfacial ionic diffusion and interface microstructure of ferroelectric/ferrite composite were investigated.

2. Experimental procedure

The specimens were prepared by the conventional oxide-mixing technique. 99% pure reagent-grade PbO, NiO, Nb_2O_5, TiO_2, Fe_2O_3, CuO, ZnO, Bi_2O_3 and MnO_2 oxides were weighed in the appropriate proportions and used as starting materials. Fe_2O_3, NiO, CuO and ZnO powders, according to the composition $(Ni_{0.5}Cu_{0.1}Zn_{0.4})Fe_2O_4$ (abbreviated as NCZ) with additive of 1 mol% Bi_2O_3, were calcined at 780°C for 4 hours to fabricate NiCuZn ferrite. The dielectric material, according to the composition $0.75Pb(Ni_{1/3}Nb_{2/3})O_3$-$0.15PbTiO_3$-$0.10Pb(Zn_{1/2}W_{1/2})O_3$ (abbreviated as PNNT) with additive of 0.5 mol% MnO_2,

*Author to whom all correspondence should be addressed.

was calcined at 800°C for 4 hours. The calcined mixtures were ground by ball milling for 12 hours to a proper surface area. The ground powders were dried and added to PVA for the disk bodies. Firstly, in order to measure characteristics such as phase structure, shrinkage percentage and sintered densities, ferroelectrics and ferrite disks were separately prepared and sintered at 800–950°C for 2 hours. Secondly, to investigate the interaction of the two materials, the 50/50 wt% mixture (designated as HH) of the PNNT ferroelectrics and NCZ ferrite powder was prepared. Finally, the calcined powders of ferroelectric and ferrite were laminated into a mould and compressed into a plate with the diameter of 12 mm and was sintered at 800°C–950°C for 2 hours.

The sintered densities were measured by the Archimedes method. The phase structure for the specimens were identified using X-ray Diffractometer (XRD). For lead-based ferroelectrics, perovskite phase and pyrochlore phase always coexists. The relative amounts of perovskite and pyrochlore phases were determined by measuring the major X-ray peak intensities for perovskite and pyrochlore phases, i.e. (110) and (222), respectively. The percentage of perovskite phase was calculated by the following equation [14]:

$$\text{Content of perovskite phase}\,(\%) = I_{\text{perov}(110)}/\left(I_{\text{perov}(110)} + I_{\text{pyroc}(222)}\right)$$

where I_{perov} and I_{pyroc} stand for the intensities of the major peaks (110) and (222) for perovskite and pyrochlore phases, respectively. The microstructure and compositional distribution on the cross section of the composites were examined by a scanning electron microscope (SEM, Hitachi, S-570), and energy-dispersive X-ray spectroscopy (EDS), respectively.

3. Results and discussion

3.1. The phase structure and sintering properties of single ferroelectrics and ferrite material

The phases and sintered densities of ferroelectrics and ferrite specimens are shown in Tables I and II, respectively. As listed in Table I, the two phases, perovskite phase and pyrochlore phase, coexist in PNNT materials, and the amounts of perovskite phase increase with increasing sintering temperature. Because the formation of lead-based ferroelectrics is by the repetition of the following reactions:

TABLE I Phase structure and sintered properties of PNNT ferroelectrics

Sintering temperature (°C)	800	850	880	900	950
Perovskite phase (%)	89.15	96.95	97.39	97.49	98.64
Pyrochlore phase (%)	10.85	3.05	2.61	2.51	1.36
Sintered density ($g \cdot cm^{-3}$)	6.42	7.55	8.01	8.13	8.15
Relative density (%)	76.43	89.93	95.36	96.79	97.02
Liner shrinkage (%)	1.50	15.11	17.61	18.13	18.17

TABLE II Phase structure and sintered properties of NCZ ferrite

Sintering temperature (°C)	800	850	880	900	950
Spinel phase (%)	100	100	100	100	100
Sintered density ($g \cdot cm^{-3}$)	3.39	4.66	5.04	5.15	5.18
Relative density (%)	63.30	86.98	94.12	96.12	96.63
Linear shrinkage (%)	5.67	14.25	16.67	17.5	17.9

$$3PbO + 2Nb_2O_5 \xrightarrow{530-600^\circ C} Pb_3Nb_4O_{13} \quad \text{(Cubic pyrochlore)} \quad (1)$$

$$Pb_3Nb_4O_{13} + PbO \xrightarrow{600-700^\circ C} 2Pb_2Nb_2O_7 \quad \text{(Rhombohedral pyrochlore)} \quad (2)$$

$$Pb_2Nb_2O_7 + 1/3XO \xrightarrow{700-800^\circ C} 1/3Pb_3Nb_4O_{13} + Pb(X_{1/3}Nb_{2/3})O_3 \quad (3)$$

where X stands for a two-valance cation, e.g., Mg^{2+}, Ni^{2+}, Zn^{2+}. The initial reaction between PbO and Nb_2O_5 results in the formation of cubic pyrochlore $Pb_3Nb_4O_7$, where upon further reaction with PbO results the formation of a rhombohedral pyrochlore $Pb_2Nb_2O_7$ (Equation 2). At last, the rhombohedral pyrochlore reacts with XO at higher temperature to form perovskite phase, with the reappearance of cubic pyrochlore phase. So it is difficult to eliminate the cubic pyrochlore phase of the type $Pb_3Nb_4O_{13}$ [15]. And it is apparent that increasing temperature causes the samples to higher density.

For NCZ ferrite samples, pure spinel phase is obtained at sintering temperature higher than 800°C. As revealed in Table II, the density of the sintered ferrite is increased as the sintering temperature is raised to 950°C. In the early stages of the densification the shrinkage is mainly due to the particle rearrangement. Then significant densification proceeds rapidly during the temperature range from 800°C to 880°C, however the process has a reduced shrinkage after the sintering temperature higher than 900°C. For example, the relative density is 63.30% at 800°C and increases to 94.12% at 880°C, finally amounts to 96.63% at 950°C. Both ferroelectrics and ferrite materials are well densified at temperature higher than 900°C. As shown in Tables I and II, the relative density can amount to ~97% at 950°C, which means that a multilayer composite of the two materials can be sintered at low temperatures and it is beneficial to use pure Ag as inner electrode for the LC filter.

3.2. The interaction of the ferroelectrics and ferrite materials

To determine whether interfacial reactions would occur or not between the two materials, the 50/50 wt% mixture of the PNNT and NCZ was prepared and sintered at 800°C–950°C for 2 hours. Table III shows the phase structure and density of mixture samples sintered at different temperature. As an example, Fig. 1 shows XRD

TABLE III Phase structure and sintered properties of mixture samples HH

Sintering temperature (°C)	800	850	880	900	950
Perovskite phase (%)	66.96	67.57	68.65	69.50	68.56
Pyrochlore phase (%)	7.54	5.41	4.89	4.43	3.62
Spinel phase (%)	25.50	27.02	26.46	26.07	27.82
Sintered density ($g \cdot cm^{-3}$)	4.39	5.77	6.16	6.27	6.37

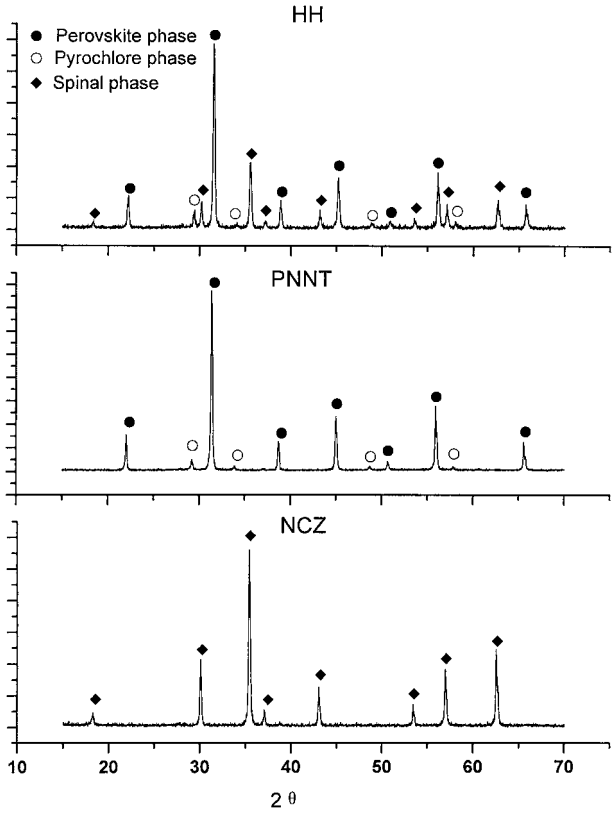

Figure 1 XRD patterns of the mixture sample, ferroelectrics and ferrite sintered at 880°C.

patterns of the mixture sample, ferroelectrics and ferrite sintered at 880°C, respectively. There are two phases, perovskite and pyrochlore phase, coexist in the PNNT ferroelectrics and only spinel phase exist in the NCZ ferrite. In the XRD pattern of the mixture sample, no other phases could be detected, except the perovskite, pyrochlore and spinel phase. From Table III, it also reveals that the density of HH samples is higher than that of the NCZ ferrite and lower than density of ferroelectrics, just between the single ferroelectrics and ferrite materials, as shown in Fig. 2. The results indicate that no chemical reaction occured for the cofired mixture, and the two materials chosen in the present study are chemical compatible.

3.3. The shrinkage properties and the camber development in ferroelectric/ferrite composites

Fig. 3 shows the shrinkage of single PNNT and NCZ materials sintered at different temperature. The trend can be summarized as follows: (1) The starting sintering

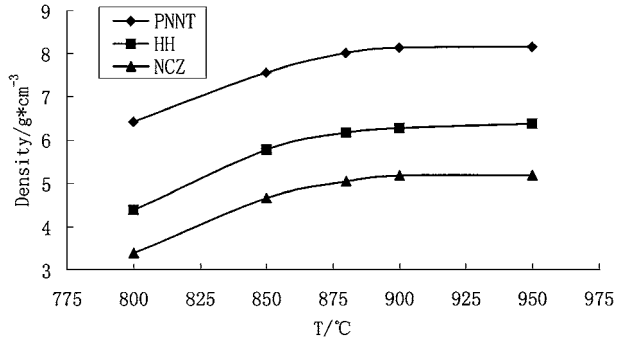

Figure 2 Densities of PNNT, NCZ and HH samples sintered at different temperature.

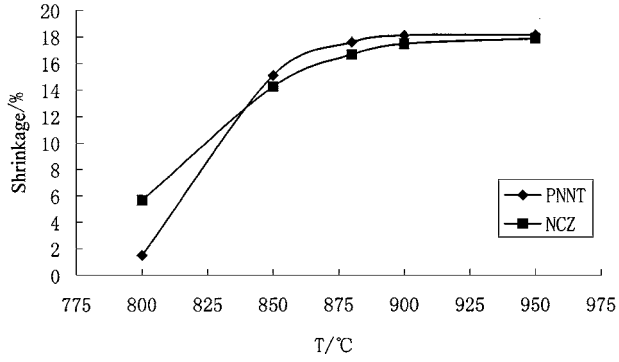

Figure 3 The shrinkage of PNNT and NCZ materials sintered at different temperature.

temperature of NCZ is lower than that of PNNT, but the densification of PNNT, once started, proceeds more rapidly than sintering of NCZ; (2) At the temperature 950°C, when the densification of the two materials finished, they reveal almost the same linear shrinkage which means that the two materials can be successfully cofired at 950°C.

To succeed in the cofiring of multilayer LC filters, the sintering behavior of the two materials must be similar. The general conditions of matching between the heterogeneous layers in the cofiring composites are related to: (1) linear shrinkage during sintering; (2) densification rates; (3) thermal expansion coefficients. It is considered that linear shrinkage mismatch is much more important than thermal expansion coefficients because linear shrinkage is in % order while thermal expansion coefficients are in ppm order. Different linear shrinkage and densification rate of the multilayer composite result in planar tensile and compressive stresses. Both such stresses lead to undesirable defects such as delamination, cracks and camber in the final products.

In fact, the camber was observed in ferroelectrics/ferrite composites because of the mismatch shrinkage at the temperature range from 800°C to 900°C. Fig. 4 depicts the camber development in sequence for ferroelectric/ferrite composites during cofiring. The camber developed through three stages, firstly the camber went toward ferrite and secondly toward ferroelectrics, finally the camber disappeared and the composites became flat.

From Fig. 3, the shrinkage of ferrite is larger than that of the ferroelectrics sintered at 800°C, and the

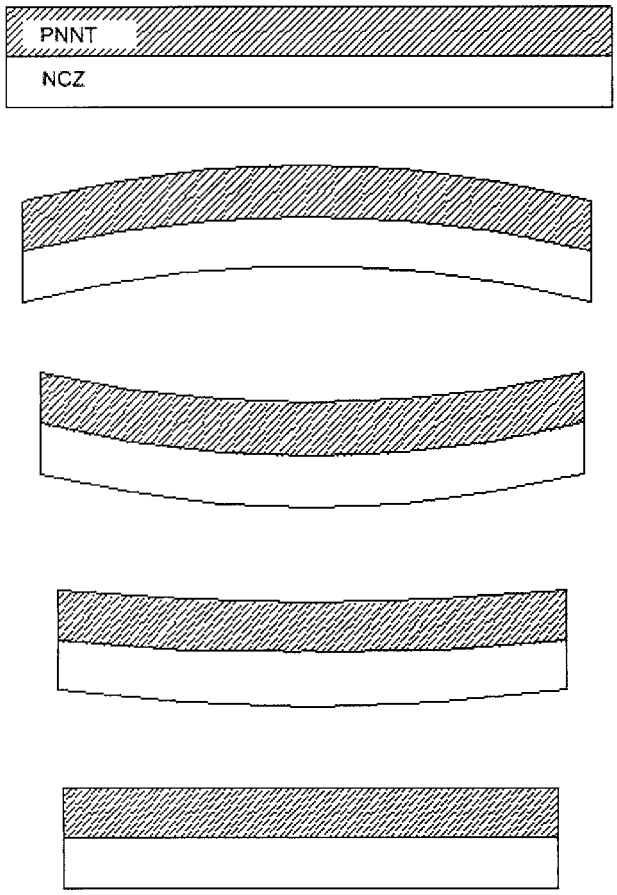

Figure 4 The camber development in sequence of ferroelectric/ferrite two-layered composites.

difference of linear shrinkage between the PNNT and NCZ leads to the camber toward ferrite. Because the densification rate of ferroelectrics is faster than that of ferrite at the temperature range from 800°C to 880°C, when the samples were sintered at the temperature range from 850°C to 900°C, it shows that PNNT materials have a larger shrinkage than NCZ ferrite, and then lead to the camber becoming downward to the PNNT ferroelectrics. Finally when the densification of the two materials finished at the temperature 950°C, the two materials reveal almost the same linear shrinkage which made the composite show no obvious camber and become flat.

The equation used to describe the camber is given as [16]:

$$\text{Cam} = \frac{(r-t)(1-\cos\theta)}{2r\sin\theta} \tag{4}$$

where t is total thickness of sintered composite, r is the camber radius, and θ is camber angle. However, it is difficult to measure the camber angle from the sintered composites. In this work, because there are no chemical reaction occurred between the PNNT and NCZ materials, it is assumed that each layer sustains its own shrinkage during the sintering process. The following equations illustrated by Fig. 5 are proposed based on the Equation 4 and applied in measuring camber as a simpler and more effective way.

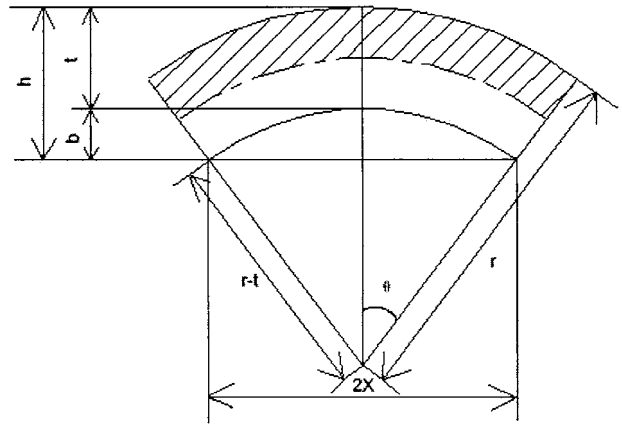

Figure 5 Configuration of the camber model after sintering.

From Fig. 5, cos and sin can be expressed as:

$$\cos\theta = \frac{r-t-b}{r-t} \tag{5}$$

$$\sin\theta = \frac{x}{r-t} \tag{6}$$

where b and x are defined as camber axial distance and camber radial distance, respectively.

It is apparent that the relation of $r-t$ with x and b is:

$$x^2 + (r-t-b)^2 = (r-t)^2 \tag{7}$$

From above equation, $r-t$ can be expressed by the function:

$$r - t = \frac{x^2+b^2}{2b} \tag{8}$$

Then the camber can be derived by Equations 5, 6, and 8 as follows:

$$\text{Cam} = \frac{b(x^2+b^2)}{2x(x^2+b^2+2bt)} \tag{9}$$

where b, $2x$ and t can be easily measured by optical microscope and the camber can be calculated by Equation 9.

Table IV shows the shrinkage difference, the calculated camber and the camber radius from the experimental data, where the positive direction of camber is defined as the camber towards to ferroelectrics while the negative sign stands for the camber towards to ferrite materials. The more the shrinkage difference is, the larger the camber and the smaller the camber radius

TABLE IV The results of calculated camber and camber radius

Sintering temperature (°C)	800	850	880	900	950
Shrinkage difference (%)	−4.17	0.86	0.94	0.63	0.27
Camber (%)	−4.08	2.44	2.98	2.31	0
$r-t$ (mm)	28.51	48.26	42.10	51.37	∞

is. In contrast, the composites sintered at 950°C show no camber because of the little difference of shrinkage, and its camber radius should be infinite.

3.4. The ionic interdiffusion and interface microstructure of the ferroelectric/ferrite composites

Interfacial microstructure analysis is performed, it should reveal any evidence of phase formation and sintering defects (i.e., delamination and cracks) because of differences in sintering kinetics. From above discussion, it indicates that the multilayer composite can be successful cofired at 950°C with no camber and interface interaction. Fig. 6 is SEM micrograph of the interfacial microstructure of ferroelectric/ferrite composite that was sintered at 950°C for 2 hours. It shows that the interface is mechanically and chemical continuously. The ferroelectrics is composed of grains 2.5–3 μm in diameter which is larger than that of ferrite (0.5–1 μm). The interface is solid, continuous with no delamination and cracks.

Then after the surface across the lamination was polished, the ionic interface diffusion was investigated by energy-dipersive X-ray spectroscopy (EDS). Fig. 7 show the distribution curves of the characteristic X-ray intensities for the ions across the interface, where A is PNNT ferroelectrics adjacent to interface and B is NCZ ferrite. It shows that the ionic diffusion occurred across the interface. For Pb^{2+}, Nb^{5+}, Ni^{2+}, Ti^{4+}, Fe^{3+}, and Zn^{2+} ions, it is revealed that there are two plates regions of constant composition operated by a region of changing composition the slopping region in the middle part of a scanning curve. It is similar to the results observed in our previous study [17]. The constant composition regions correspond to the ionic concentration in ferroelectrics and ferrite. The sloping region is the ionic interdiffusion area across the interface between PNNT and NCZ. Different ions have slightly different thickness of interdiffusion layers; the interdiffusion layer is typically 10 μm thick. Because of the strong ionic diffusion across the interface of the two materials, no distinct separation layer observed between them, which is beneficial to low-temperature-cofiring multilayer LC filter.

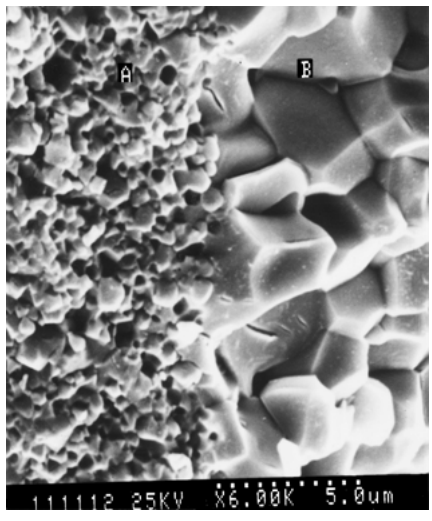

Figure 6 SEM micrograph of the interface between ferrite (A) and ferroelectrics (B) materials.

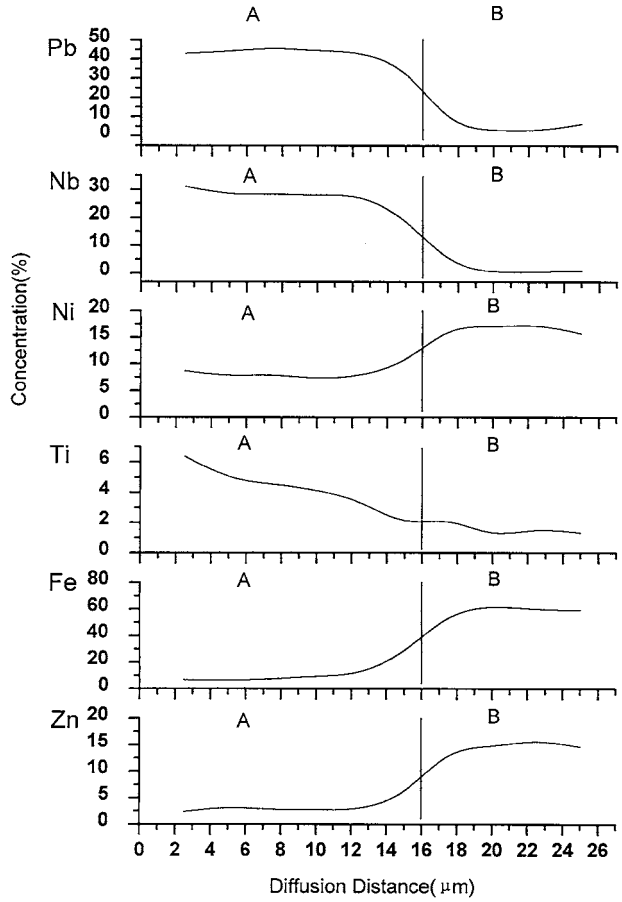

Figure 7 Typical distribution curves of the characteristic X-ray intensities from PNNT (A) to NCZ (B) for different ions (950°C/2 h).

4. Conclusion

In summary, through the investigation of the densification characteristics of the single ferroelectrics and ferrite materials, the multilayer ferroelectric/ferrite composites were prepared and camber development, interfacial ionic diffusion and interface microstructure were investigated. The results show that no chemical reaction occured for the ferroelectrics and ferrite, and the two materials chosen in the present study are chemical compatible. The camber of the composites were observed because of mismatch shrinkage at the temperature range from 800°C to 900°C. It is shown that the camber developed firstly toward ferrite and secondly toward ferroelectrics, finally disappeared and the composites became flat at 950°C. The multilayer ferroelectric/ferrite composites can be successfully cofired at 950°C and the interface is continuous with no delamination and cracks, which should attribute to the strong ionic diffusion across the interface of the two materials.

Acknowledgment

This work is supported by the Doctorate Foundation of Northwestern Polytechnical University.

References

1. JAU-HO JEAN and CHIA-RUEY CHANG, *J. Amer. Ceram. Soc.* **80**(12) (1997) 3084.
2. FRANCIS J. TOAL, JOSEPH P. DOUGHERTY and CLIVE A. RANDALL, *ibid.* **81**(9) (1998) 2371.
3. HSIAO-MIIN SUNG, CHI-JEN CHEN, LIH-JIUN WANG and WEN-SONG KO, *IEEE Trans. Magn.* **34**(4) (1998) 1363.
4. JEN-YAN HSU, HON-CHIN LIN, KUN-FU FU and HON-DAR SHEN, in "Multilayer Electronic Ceramic Devices," edited by Jau-Ho Jean, T. K. Gupta, K. M. Nair and K. Niwa (1998) p. 253.
5. SHENG-YUAN CHU and CHENG-SHUNG HSICH, *J. Mater. Letter.* **19** (2000) 609.
6. A. VIERHEILIG and A. SAFARI, *Ferroelectrics* **135** (1992) 147.
7. LIJIAN RUAN, LONGTU LI and ZHILUN GUI, *J. Mater. Letter.* **16** (1997) 1020.
8. ATSUYUKI NAKANO and TAKESHI NOMURA, in "Multilayer Electronic Ceramic Devices," edited by Jau-Ho Jean, T. K. Gupta, K. M. Nair and K. Niwa (1998) p. 285.
9. S. H. SEO and J. H. OH, *IEEE Trans. Magn.* **35**(5) (1999) 3412.
10. J. H. JEAN and C. H. LEE, *Jpn. J. Appl. Phys.* **38** (1999) 3508.
11. GUO-QUAN LU, ROBERT C. SUTTERLIN and TAPAN K. GUPTA, *J. Amer. Ceram. Soc.* **76**(8) (1993) 1907.
12. JAU-HO JEAN, CHIA-RUEY CHANG and ZHIEN-CHI, *ibid.* **80**(9) (1997) 2401.
13. CHIA-RUEY CHANG and JAU-HO JEAN, *ibid.* **81**(11) (1998) 2805.
14. SANG-GU KANG, HWAN KIM and JONG-KOOK LEE, *J. Mater. Sci.* **32** (1997) 5377.
15. THOMAS R. SHROUT and ARVIND HALLIYAL, *Amer. Ceram. Soc. Bull.* **66**(4) (1987) 704.
16. HYO TAE KIM, SANG KI KO and YOONHO KIM, in "Multilayer Electronic Ceramic Devices," edited by Jau-Ho Jean, T. K. Gupta, K. M. Nair and K. Niwa (1998) p. 241.
17. GAO FENG, QU SHAOBO, YANG ZUPEI, TIAN CHANGSHENG, *J. Mater. Letter.* **21**(1) (2002) 15.

Received 25 January
and accepted 16 December 2002